Analysis of Crustal Structure in the region of Ribeira Belt (between the Provinces of the São Francisco Craton and the Paraná Basin) using Seismological Methods.

Diogo Luiz de Oliveira Coelho, Stéphane Drouet, Observatório Nacional, Rio de Janeiro, Brazil

Abstract

The work area covering the north of São Paulo, South of Rio de Janeiro e South of Minas Gerais. Our study have as main goal generate images of crustal discontinuities. With these images we intend add information about the local geological framework, corroborating for delineate with accuracy the discontinuities. Were installed twenty four seismograph stations in three sections, two perpendiculars to coast and one parallel. The distance between the stations is approximately 20 km. The first analysis done is noise level and to calculate a regional crustal thickness was used the method called Receiver Function. To obtain a image of discontinuities, as Moho, the stacking of Receiver Functions are mapped in relation to station position in the section. The calculated values of the Moho depth for each station were linearly interpolated to generate a regional map. We see the Moho thinning in direction to east, reinforcing the proximity with the oceanic crust.

Introduction

The work area is found in the geographic quadrant sited between the coordenates north (21°19'5" S/45°39'31" W e 22°7'59" S/46°54'23" W) and south (23°8'28" S/48°13'28" and 23°57'33" S/45°28'35" W) covering the north of São Paulo, South of Rio de Janeiro e South of Minas Gerais. Localized near the cities like: Parati-RJ; Guaratinguetá-SP; Taubaté-SP; Ubatuba-SP; São José dos Campos-SP; Caraguatatuba-SP; São Gonçalo do Sapucaí-MG; Itajubá-MG; Alfenas-MG; Varginha-MG; Pouso Alegre-MG. The Total area of this project is the approximately 33600 km^2.

The study area is enframed geologically in Continental Rift of the Southeast of Brazil over polycyclic terrains referable to south of the Ribeira Belt, as Riccomini (1990) cites in your paper. This Belt is compound for metamorphic rocks, migmatites and granitoids related to Brasiliano Orogenetic Cycle. This geological zone is titled for Almeida and Carneiro (1998) as Planalto Atlantico. The area is found on a region reworked by preterite orogenic cycles and the lithological set was intruded by transcorrents thrust systems oriented according to regional trend, direction ENE to EW, in accordance with Hasui and Sadowski (1976).

The main goal is generate images of the crustal discontinuities. With these images, we intend add information about the local geological framework, corroborating for delineate with accuracy the discontinuities.

Methodology

Were installed twenty four seismograph stations in three sections, two perpendiculars to coast and one parallel, as observed in Figure 1. The section 1 extends from the STA01 station, located near the coast, to STA09. The section 2 goes of station STA10, north, to station STA16, near the coast. Section 3 extends from station STA17, west, to station STA24, east. The distance between the stations is approximately 20 km.

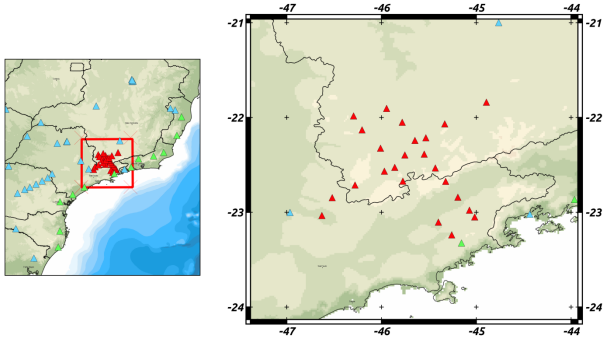

Figure 1: Map of the seismograph stations installed (red triangles). The others triangles are of the Brazilian Seismographic Net.

The seismographs are broadband (STS2 ou Reftek RT151-120s) and the record frequency band is at interval 50 Hz - 100 seconds. The perpendicular sections were installed in half of 2012 and parallel section in the end of 2012. The stations ran until the end of 2013 registering the terrain movement.

The first analysis done was the mensuration of noise level in the stations using PQLX software. The calculus of noise level is based in the work of McNamara and Buland (2004). The data was separated in intervals of one hour with 50% of superposition. Each interval was separated in 13 parts with 75% of superposition to calcule a "Power Spectral Density". Later was partitioned in 13 parts with 75% of superposition to calculate a "Power Spectral Density". The obtained means for each one of 13 parts are used to estimate a "Probability Density Functions" that are

estimates by the calculus of the means for the total number of hourly interval.

This method differs of others utilized because is not necessary display the data to remove the existing noise. The noise is compound by calibration seisms, cultural noise, instrumental problems and a lack of data. These types of noise have a low Probability Density Functions, according McNamara and Buland (2004), then is suppressed.

To calculate a regional crustal thickness was used the method called Receiver Function, that was developed for Langston (1977). That method use the signal of teleseisms, generators of plane waves of quasi-vertical incidence beneath a given station. The P wave arrival in the Mohorovicic seismic discontinuity, also known as Moho, and decomposes in a transmitted P wave e a converted S wave. The difference of arrival time of both waves and of others reflections allows infer Moho thickness, as observed in the Figure 2.

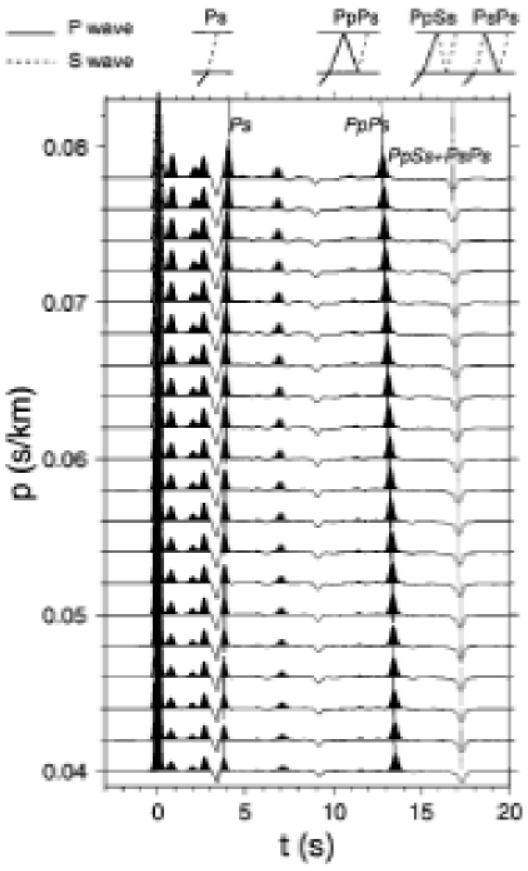

Figure 2: Synthetic Receiver Fuction
(Zhu and Kanamori, 2000)

Seisms near of station, distance less than 20 degrees, generate waves with oblique incidence and this data type should be utilized with careful. In seisms with distances bigger than 95 degrees, the P waves don't arrive in station due to the velocity inversion in the mantle-core boundary. Another important fact is that cannot observed a direct P wave.

The Receiver Functions are calculated with a deconvolution in time-domain of the radial component by the vertical component. This eliminates similar parts of signals, source and source's propagation until Moho. The Receiver Function is sensible in the delimitation of crustal superficial structuration under the station. The software SAC (*Seismic Analysis Code*) was used to process and to calculate the Receiver Functions.

A robust method to analyse the Receiver Functions is the method of Zhu and Kanamori (2000). Using the medians velocities in the crust, the time differences between P wave and a converted P wave in S can be calculated, as well as the time of multiples.

$$H = \frac{t_{P_s}}{\sqrt{\frac{1}{v_s^2} - p^2} - \sqrt{s\frac{1}{v_p^2} - p^2}} \quad (1)$$

$$H = \frac{t_{P_pP_s}}{\sqrt{\frac{1}{v_s^2} - p^2} + \sqrt{\frac{1}{v_p^2} - p^2}} \quad (2)$$

$$H = \frac{t_{P_pS_s} + t_{P_sP_s}}{2\sqrt{\frac{1}{v_s^2} - p^2}} \quad (3)$$

Using a given velocity v_p, the arrival times can be calculate with the Moho thickness(H), the v_p/v_s ratio and the ray parameter, this depends of location and depth of the event. Rather than trying to adjust all the function, the method make a search,*grid search*, of the crustal thickness and the v_p/v_s ratio to calculate the theoretical arrival times of the converted P waves in S and your multiples for each register. The best combination of crustal thickness and v_p/v_s ratio is one that maximizes the value of the real amplitudes of the Receiver Functions.

To obtain a image of discontinuities, as Moho, the stacking of Receiver Functions are mapped in relation to station position in the section. The data are divided in 4 groups, according the azimuth between the seism and the station. The majority of the events occur in the northwest and southwest region, we can note a scarcity of quakes in the region of Atlantic Ocean. The goal of this separation is evaluate if exist lateral variation of structure.

Results

The Figure 3 shows the registered events in STA08 station. The most part of seisms recorded in stations are events from Andes range or Central America.

The results from the Figure 4 allows a fast evaluation of the data quality. We observed some curves diverging with the superior and inferior bounds of noise, but are punctual events with a low probability (violet curves). In majority of stations the curves were found in the intermediary zone, shown a data quality good to moderate.

In some stations, high probabilities appear in short and long period. This is related with diurnal variations. These changes are connected with human activity (short period) and temperature (long period). In general, the noise of short period is compound for noise generated in humans activities, with interval between 1 and 15 seconds, as shown in Figure 4. This noise type is dominated for micro-seisms. In noise of long period (>30 s) the influence of

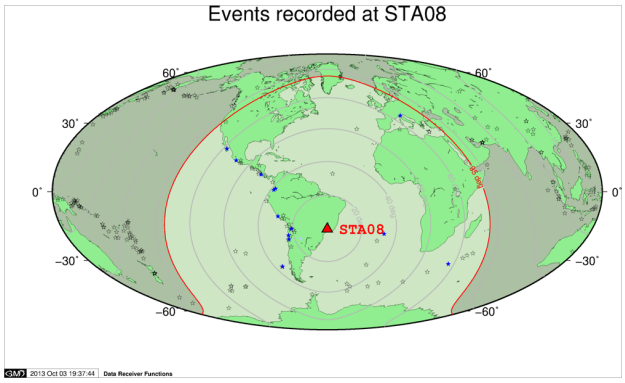

Figure 3: Map with recorded events by STA08 station. The red triangle represents the station and the blue stars represent the seisms.

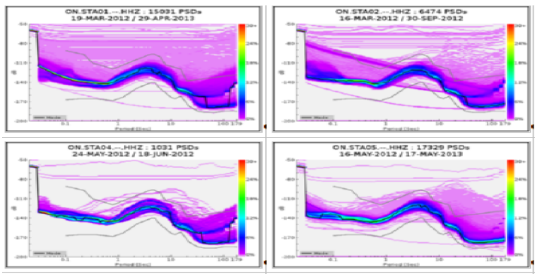

Figure 4: Examples of evaluation of data quality by the method of McNamara and Buland (2004)

atmospheric pressure variation and temperature can alter the noise level. In case of temporary installation, the thermic isolation is basic, which carries a high level of long period noise. The quakes generate signal of high frequency (1-10 Hz), in case of local or regional seisms, already the teleseisms are of long period (10-20 seconds).

The Figure 5 shows a section of Receiver Functions obtained from several events and normalized by the amplitude of the first peak. The first peak is the direct P-wave arrival, the second highest, around 5 seconds, is the P wave converted to S wave in the Moho discontinuity.

The multiples PpPs e PpSs+PsPs not have a high amplitude. The Figure 5 shows also the deconvolution of transversal component by the vertical component.Assuming a medium, without lateral variation, the deconvolution should be zero. The small amplitude of transversal component suggests a little lateral alteration in the properties of medium. To amplify the signal-noise ratio of second peak in Receiver Functions a simple stacking of all functions was realized. After, the data separation in four groups divided by the azimuth between the quake and the station.

We noted in Figure 6 a substantial subsidence under the station STA04. We realized signals before the Moho, among 2 and 4 seconds, who have a depth variations along the profile. This can be related to interfaces with a contrast of different physical property. The negative pulse, red color, indicates an existence of a low-velocity layer. According with geological setting, we can infer that layer is the Taubatè basin, because this basin is located in a rift

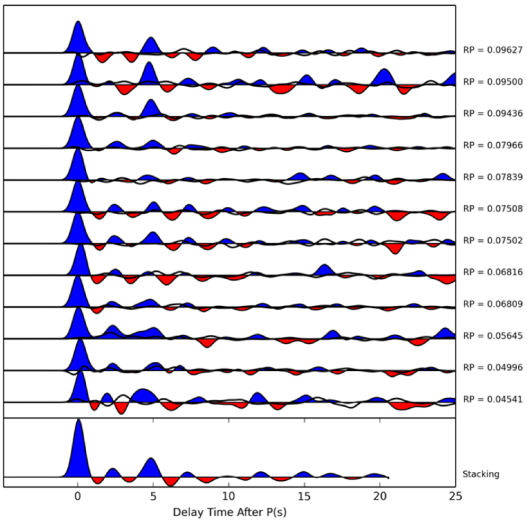

Figure 5: Receiver Functions calculated to the STA08 station and the simple stacking.

system, and this explain the subsidence of Mantle.

We calculated the crustal thickness (H) that maximizes the value of real amplitudes of Receiver Function. The best combination of crustal thickness and v_p/v_s ratio calculated for each station is found in Table 1. The solutions found corroborate with the results from Assumpção et al. (2013b), Assumpção et al. (2013a) and van der Meijde et al. (2013) in data of compilations from works of South America and Brazil. The obtained values for crustal thickness in Table 1 are according with the mean measured by Assumpção et al. (2013b), Assumpção et al. (2013a) and van der Meijde et al. (2013), is about 30 40 km.

The uncertainty, shown in Table 1 are linked to quality and quantity of the Receiver Functions. A important phase is the selection of the best Receiver Functions, because the data quality is preponderant over the quantity. The uncertainty associated a each one of obtained parameters by the method Hk and estimated generally by ”bootstrap” method, developed for (Efron and Tibshirani, 1991). From the original set of Receiver Functions the program generates subsets containing traces randomly selected. These method is repeated for each subsets, resulting in a parameter set H and v_p/v_s .Mean and standard deviation from the values provide us a mean value and an estimate of the uncertainty associated to determination. There is no rule for determining the number subsets that must be generated, the crucial is search a value that makes the estimative stabilize, including uncertainties. In general we use a value between 100 and 200 subsets depending on the amount de traces available during the “bootstrap”.

The calculated values of the Moho depth for each station were linearly interpolated to generate a regional map, shown in the Figure 7. To improve the interpolation, we added data from (Assumpção et al., 2013a). In the Figure 7 we can see the Moho thinning in direction to east, reinforcing the proximity with the oceanic crust.

Table 1: Table with crustal thickness and v_p/v_s ratio.

Station	Altitude	Latitude	Longitude	Depth	Uncertainty	Vp/Vs ratio	Uncertainty	Number
STA01	-23.049408	-45.016808	950	35.4000	3.1246	1.7500	5.96E-002	5
STA02	-22.977707	-45.072017	886	35.6000	1.5851	1.7200	4.28E-002	15
STA03	-22.840839	-45.194141	576	35.0000	8.3778	1.7300	9.84E-002	19
STA04	-22.673525	-45.323162	902	37.0000	7.2112	1.7400	1.23E-001	6
STA05	-22.5325	-45.432383	1100	41.0000	6.9241	1.6700	1.62E-001	29
STA06	-22.386261	-45.549086	931	55.2000	30.9314	1.7900	1.05E-001	8
STA07	-22.241667	-45.647361	988	38.8000	1.7971	1.7000	4.80E-002	24
STA08	-22.050056	-45.781374	884	33.2000	6.3031	1.8500	1.33E-001	22
STA09	-21.903929	-45.946331	1045	42.6000	4.3086	1.6800	8.77E-002	30
STA10	-21.98335	-46.29471	1135	38.8000	3.9148	1.7500	7.05E-002	5
STA11	-22.12999	-46.20536	1455	41.0000	4.2658	1.7100	9.04E-002	11
STA12	-22.32379	-46.01047	890	37.4000	0.6134	1.7700	1.52E-002	25
STA13	-22.52571	-45.86029	918	35.8000	3.2668	1.7800	7.67E-002	13
STA14	-22.67147	-45.77467	974	38.0000	2.9979	1.8000	7.40E-002	12
STA15	-23.10378	-45.39983	895	35.8000	0.8721	1.7400	3.26E-002	6
STA16	-23.2387	-45.25919	906	32.2000	4.1659	1.8000	1.06E-001	7
STA17	-23.0337	-46.62914	776	37.8000	1.5258	1.6900	4.39E-002	6
STA18	-22.84539	-46.52033	957	41.0000	8.0172	1.7200	1.32E-001	5
STA19	-22.71192	-46.27943	1413	39.0000	2.5130	1.7500	6.23E-002	18
STA20	-22.56621	-45.96951	908	38.2000	4.1389	1.7500	8.20E-002	11
STA21	-22.39548	-45.75364	957	39.0000	4.8590	1.7200	1.07E-001	9

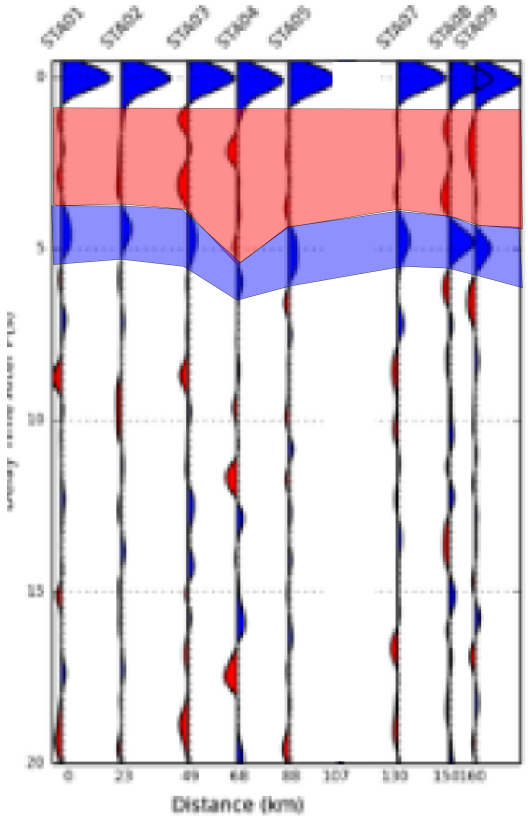

Figure 6: Section of Receiver Functions

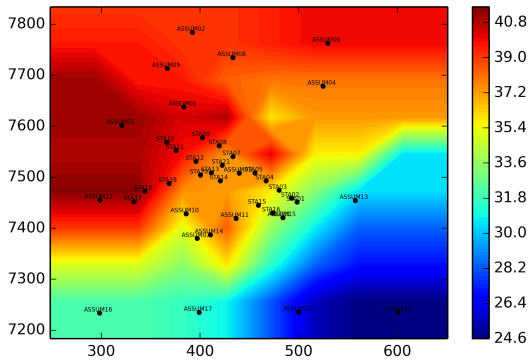

Figure 7: Linear Interpolation of Moho depth of each station more data from (Assumpção et al., 2013a)

Conclusions

The data analysis indicate same preliminary results about the Moho depth in the region between São Paulo, Minas Gerais and Rio de Janeiro. The Receiver Functions also assist to establish a image of the Crustal Framework. The generated images show a thinning trend in East direction, boundary of the continental crust.

References

Almeida, F. F. M. D., and C. D. R. Carneiro, 1998, Origem e evolução da serra do mar: RBG, **28**, 135–150.

Assumpção, M., M. Bianchi, J. Julià, F. L. Dias, G. Sand França, R. Nascimento, S. Drouet, C. G. Pavão, D. F. Albuquerque, and A. E. V. Lopes, 2013a, Crustal thickness map of brazil: Data compilation and main features: Journal of South American Earth Sciences, **43**, 74–85.

Assumpção, M., M. Feng, A. Tassara, and J. Julià, 2013b, Models of crustal thickness for south america from

seismic refraction, receiver functions and surface wave tomography: Tectonophysics, **609**, 82–96.
Efron, B., and R. Tibshirani, 1991, Statistical data analysis in the computer age: Science, **253**, 390–395. (PMID: 17746394).
Hasui, Y., and G. R. Sadowski, 1976, Evolução geológica do precambriano na região sudeste do estado de são paulo: Brazilian Journal of Geology, **6**, 182–200.
Langston, C. A., 1977, The effect of planar dipping structure on source and receiver responses for constant ray parameter: Bulletin of the Seismological Society of America, **67**, 1029–1050.
McNamara, D. E., and R. P. Buland, 2004, Ambient noise levels in the continental united states: Bulletin of the Seismological Society of America, **94**, 1517–1527.
Riccomini, C., 1990, O rift continental do sudeste do brasil: text, Universidade de São Paulo. (Tese de Doutorado).
van der Meijde, M., J. Julià, and M. Assumpção, 2013, Gravity derived moho for south america: Tectonophysics, **609**, 456–467.
Zhu, L., and H. Kanamori, 2000, Moho depth variation in southern california from teleseismic receiver functions: J. Geophys. Res., **105**, 2969–2980.

Acknowledgments

The authors wish to express their gratitude to Observatório Nacional and Seismographic Network for available the research data.